論 文 内 容 の 要 旨

1. Introduction

Metal oxide nanomaterials play important roles in many fields, such as physics, chemistry, materials science, and biology, due to their unique properties originated from the nanosize, large surface area, and quantum effect, etc. The physical and chemical properties, for example chemical reactivity, surface area, porosity, and band gap energy of nanomaterials, can be tuned by controlling their sizes in nano-level. To this end, much efforts has been paid to the synthesis of size- and morphology-controlled nanomaterials by chemical methods, such as sol-gel, precipitation, microemulsion, and template synthesis. However, those chemical methods usually require multi-step reactions including long reaction time as well as calcination. Therefore, development of simple synthetic methods to yield size, composition, and morphology controlled nanomaterials is quite of importance.

Previously, Wang et al. reported a simple, rapid, one-pot, single-step, and template free synthetic method of spherical mesoporous assemblies of TiO_2 nanoparticles called **m**icro/**m**esoporously **a**rchitected **r**oundly **i**ntegrated **m**etal **o**xides (MARIMOs) due to their similarity in shape to *marimo* (*cladophora aegagropila*) moss balls,[1)] where a large number of fine primary nanoparticles ranging in the size 5–10 nm assembled affording a porous spherical secondary structure with a large specific surface area. In this solvothermal method, a precursor solution of a metal alkoxide and a carboxylic acid in methanol is simply treated under high-temperature and high-pressure conditions in a closed tubular reactor. TiO_2 solid and hollow MARIMO assemblies with narrow size distribution were easily synthesized by controlling the reaction parameters such as a sort of carboxylic acid, heating rate, and reaction temperature (Figure 1). Solid MARIMO families of SiO_2, ZnO, ZrO_2, and CeO_2 were also obtained according to the similar treatments of suitable precursors.

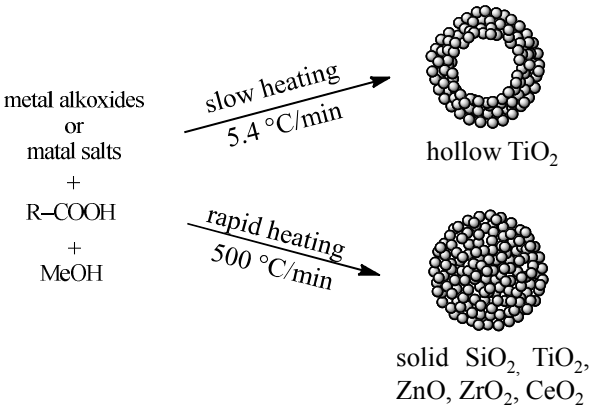

Figure 1. Synthesis of solid and hollow MARIMO assemblies by one-pot single-step method.

On the other hand, physical, chemical, and electrical properties of metal oxide materials can be improved by nano-level mixing of several metal oxides, where the stoichiometries, particle sizes, nano-structures, and morphologies are key factors controlling the properties of the resulting composite nanomaterials. In my study, I synthesized Al_2O_3–TiO_2, ZnO–TiO_2 and CeO_2–ZrO_2 composite assemblies with different distributions of primary nanoparticles such as homogeneous, domain, and core-shell structures. Moreover, MgO ultra-fine nanocrystals were synthesized by choosing suitable magnesium salts, solvents, organic additives, and reaction temperature.

2. A simple solvothermal approach to Al_2O_3–TiO_2 and ZnO–TiO_2 mesoporous hollow composite assemblies.

Mesoporous hollow nanomaterials containing composite metal oxides such as Al_2O_3–TiO_2 and ZnO–TiO_2 are quite of interest due to their intriguing morphology capable of material accommodation and the advantageous synergistic effects between two metal oxides. Al_2O_3–TiO_2 composite materials are reported to exhibit high heat tolerance for the anatase-to-rutile phase transition, and ZnO–TiO_2 composite materials are used for band gap energy tuning. However, the synthesis of Al_2O_3–TiO_2 and ZnO–TiO_2 porous composite assemblies with hollow spherical morphologies permitting the effective control of their compositions has not been intensively studied. In this chapter, one-pot, single-step, and template-free solvothermal synthetic method to lead Al_2O_3–TiO_2 and ZnO–TiO_2 MARIMO hollow spherical assemblies consisting of Al_2O_3 and ZnO fine primary nano–particles mixed with TiO_2 domains, respectively, is discussed.

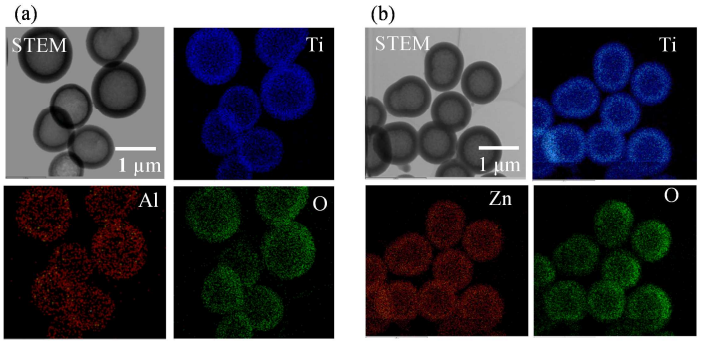

Figure 2. STEM and EDX mapping images of (a) Al/Ti–0.20 and (b) Zn/Ti–0.20 hollow MARIMO composite assemblies.

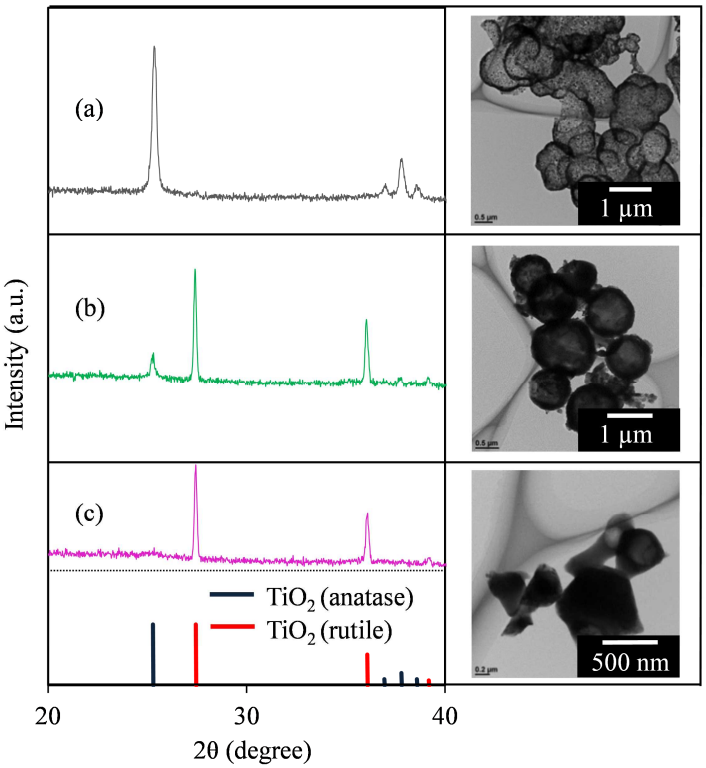

Figure 3. XRD patterns (left) and TEM images (right) of (a) Al/Ti–0.50, (b) Al/Ti–0.25, and (c) Al/Ti–0.05 hollow composite assemblies after calcination at 1,000 °C for 1 h.

Al_2O_3–TiO_2 composite assemblies were synthesized by slowly heating (5.4 °C/min, up to 300 °C) of precursor solutions consisting of $Al(O^iPr)_3$, $Ti(O^iPr)_4$, and phthalic acid in methanol with different Al/Ti mixing ratios. The obtained Al_2O_3–TiO_2 hollow composite assemblies are referred to as Al/Ti–0.75, Al/Ti–0.50, Al/Ti–0.25, Al/Ti–0.20, Al/Ti–0.10, and Al/Ti–0.05, where the numbers denote the molar portion of $Al(O^iPr)_3/(Al(O^iPr)_3 + Ti(O^iPr)_4)$ in the precursor solutions. The STEM/EDX mapping images of Al/Ti–0.20 indicate the even distribution of Al and Ti atoms throughout the hollow composite MARIMO assemblies (Figure 2a). A linear relationship between the atomic compositions of the Al_2O_3–TiO_2 hollow composite assemblies (determined by EDX) and the molar ratios of the precursor solutions was observed, indicating that the composition of the

Al_2O_3–TiO_2 hollow composite assemblies can be easily controlled by adjusting the Al/Ti mixing ratio in the precursor solutions. XRD patterns showed that the synthesized porous composite assemblies consist of anatase TiO_2 and amorphous Al_2O_3. In particular, it is notable that the BET specific surface area of Al/Ti–0.75 and Al/Ti–0.50 exceeded 600 m^2 g^{-1}.

The Al_2O_3–TiO_2 hollow composite assemblies were calcinated at 1,000 °C for 1 h to evaluate their heat properties. The XRD patterns and TEM images of calcinated Al_2O_3–TiO_2 composite assemblies are shown in Figure 6. Al/Ti–0.05 clearly showed the anatase-to-rutile phase transition and hollow spherical morphology was damaged (Figure 3c). The partial formation of the rutile phase was observed for Al/Ti–0.25 under similar conditions, while the anatase phase still remained (Figure 3b). However, in the case of Al/Ti–0.50, the anatase phase survived completely with no rutile phase formation. The hollow composite assemblies calcinated at 1,000 °C clearly indicate that the spherical hollow morphology of composite assemblies with Al = 25–50% remains intact even after the calcination at 1,000 °C for 1h (Figure 3a).

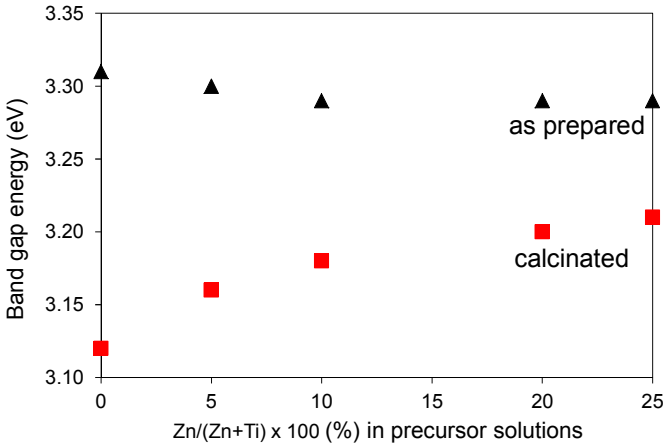

Figure 4. Plots of band gap energies of ZnO–TiO_2 hollow composite assemblies versus the initial molar fractions of Zn in precursor solutions.

ZnO–TiO_2 hollow composite assemblies referred to as Zn/Ti–0.75, Zn/Ti–0.50, Zn/Ti–0.25, Zn/Ti–0.20, Zn/Ti–0.10, and Zn/Ti–0.05, where each number denotes the molar portion of $Zn(OAc)_2/(Zn(OAc)_2 + Ti(O^iPr)_4)$ in the precursor solutions, were also obtained by a similar solvothermal method. STEM/EDX mapping images of Zn/Ti–0.20 (Figure 2b) indicate the even distribution of Zn and Ti atoms throughout the MARIMO hollow composite assemblies. The band gap energies of ZnO–TiO_2 MARIMO composite assemblies were tunable by changing the ZnO/TiO_2 mixing ratio in the assemblies. The band gap energies of the as prepared ZnO–TiO_2 composites were around 3.3 eV. However, the calcination at 500 °C for 1 h caused relatively large shifts in band gap energies to lower values of 3.12–3.21 eV (Figure 4).

3. Synthesis of CeO_2–ZrO_2 mixed mesoporous spherical nanomaterials with homogeneous, domain, and core-shell morphologies.

Much attention has been paid to CeO_2 nanomaterials for their many applications such as oxygen storage, polishing materials, catalysts, and catalyst supports. However, decreasing the amount of the rare earth metal Ce without losing its performance has become a crucial aspect of current research because of the Ce resource limitation. The synthesis of CeO_2–ZrO_2 composites is one approach to minimize Ce loading on nanomaterials. In this chapter, a simple and rapid synthetic approach to CeO_2–ZrO_2 MARIMO composite assemblies with homogeneously dispersed, domain, and core-shell structures having mesoporous spherical morphologies is discussed.

CeO_2–ZrO_2 MARIMO composite assemblies were synthesized by a similar solvothermal approach treating precursor solutions containing $Ce(NO_3)_3$ and $ZrO(NO_3)_2$ with formic acid in methanol by means of rapid heating (500 °C/min, up to 300°C). These MARIMO composite assemblies referred to as Ce/ZrO_2–0.25, Ce/ZrO_2–0.33, Ce/ZrO_2–0.50, Ce/ZrO_2–0.66, where the number designates the molar portion $[Ce^{3+}]/([Ce^{3+}] + [Zr^{4+}])$ in the precursor solutions. The TEM and EDX mapping images (Figure 5a) of Ce/ZrO_2–0.50 sample indicated the formation of MARIMO assemblies in which Ce and Zr atoms were evenly distributed. In the XRD patterns of the Ce/ZrO_2 MARIMO assemblies, the continuous shifting of the diffraction peak positions and lattice parametrs from those of CeO_2 to ZrO_2, depending on the Ce/Zr ratio in the precursor solutions (Figuress 6a-f), was observed. Judging from the TEM images and XRD patterns, the synthesis of *homogenious* $Ce_xZr_{1-x}O_2$ MARIMO assemblies were accomplished and the control of their compositions were sucessfully achieved by this simple method.

On the other hand, the sample CeO_2-ZrO_2-SH were obtained by slow heating (5.4 °C/min, up to 300 °C) of an equimolar mixture of $Ce(NO_3)_3$ and $ZrO(NO_3)_2$ with formic acid in methanol. The EDX mapping images showed that Ce, Zr, and O atoms were evenly distributed in CeO_2–ZrO_2-SH MARIMO composite assemblies (Figure 5b), while the XRD exhibited a mixed profile of cubic CeO_2 and tetragonal ZrO_2 phases (Figure 6g), indicating that CeO_2–ZrO_2-SH MARIMO composite assemblies consist of a *domain* structure with cubic CeO_2 and tetragonal ZrO_2.

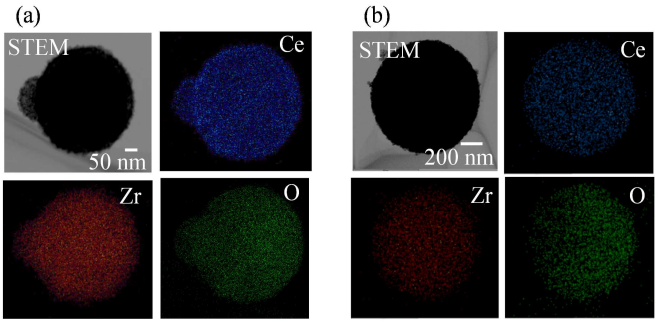

Figure 5. STEM and EDX mapping images of (a) Ce/ZrO_2–0.50 and (b) CeO_2–ZrO_2-SH MARIMO composite assemblies.

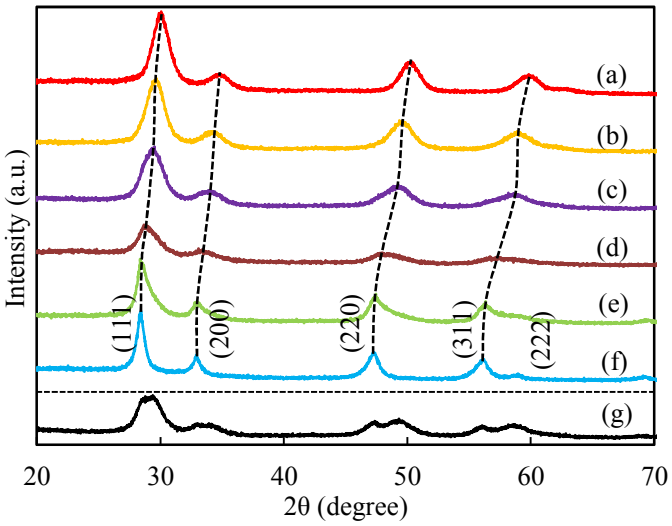

Figure 6. XRD patterns of MARIMO NPs: (a) ZrO_2, (b) Ce/ZrO_2-0.25, (c) Ce/ZrO_2-0.33, (d) Ce/ZrO_2-0.50, (e) Ce/ZrO_2-0.66, (f) CeO_2, and (g) CeO_2-ZrO_2-SH

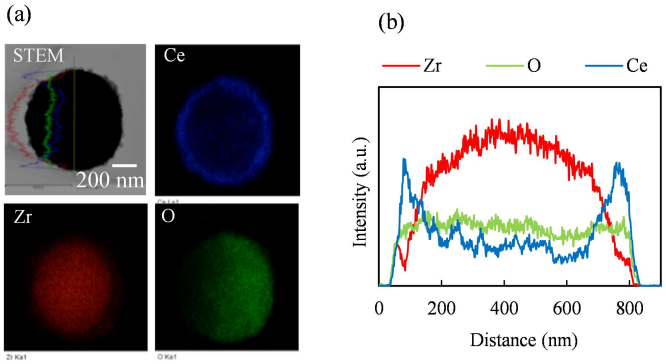

Figure 7. EDX (a) mapping images and (b) line scans of ZrO_2@CeO_2 core-shell MARIMO composite assemblies.

A step-wise synthetic approach yielded ZrO_2@CeO_2 *core-shell* MARIMO assemblies with a ZrO_2 core and a CeO_2 shell (Figure 7) by the high-temperature and high-pressure treatment of ZrO_2 MARIMO assemblies with a solution of $Ce(NO_3)_3$ in 2-propanol.

4. Synthesis of Mg-nanomaterials

Mg-nanomaterials were successfully synthesized by our solvothermal method.

5. Conclusions

A simple synthetic method to afford Al_2O_3–TiO_2 and ZnO–TiO_2 hollow composite assemblies was developed. Atomic compositions in Al_2O_3–TiO_2 and ZnO–TiO_2 hollow composite assemblies were controllable through the mixing ratio of the corresponding metal sources in the precursor solutions. Al_2O_3–TiO_2 hollow composite assemblies with high Al content (Al = 50%) did not show any phase transition from anatase-to-rutile even after calcination at 1,000 °C for 1 h. The band gap energy of TiO_2 in ZnO–TiO_2 assemblies was tuned by changing their ZnO content. A simple synthetic method to afford CeO_2–ZrO_2 porous spherical composite assemblies was also developed. Homogeneous, domain, and core-shell structures of CeO_2–ZrO_2 porous spherical composite assemblies were easily obtained by tuning the solvothermal conditions of solvents, organic additives, and heating rate. Atomic compositions in homogenous CeO_2–ZrO_2 porous spherical composite assemblies were also controllable through the Ce/Zr mixing ratio in precursor solutions. Moreover, Mg-nanomaterials were successfully synthesized.

6. References

1) P. Wang, K. Kobiro, Synthetic versatility of nanoparticles: A new, rapid, one-pot, single-step synthetic approach to spherical mesoporous (metal) oxide nanoparticles using supercritical alcohols, *Pure Appl. Chem.* **2014**, *86*, 785–800.

List of works

Publications

1. **E. K. C. Pradeep**, T. Habu, H. Tooriyama, M. Ohtani, K. Kobiro, Ultra-simple synthetic approach to the fabrication of CeO_2–ZrO_2 mixed nanoparticles into homogeneous, domain, and core–shell structures in mesoporous spherical morphologies using supercritical alcohols, *J. Supercrit. Fluids* **2015**, *97*, 217–223.
2. **E. K. C. Pradeep**, M. Ohtani, K. Kobiro, A simple synthetic approach to Al_2O_3–TiO_2 and ZnO–TiO_2 mesoporous hollow composite assemblies consisting of homogeneously mixed primary particles at the nano level, *Eur. J. Inorg. Chem.*, **2015**, 5621–5627.

Presentations

1. **E. K. C. Pradeep**, T. Habu, H. Tooriyama, M. Ohtani, K. Kobiro, Composition and morphology control of CeO_2-ZrO_2 composites, *高知化学会第 27 回研究会講演会*, 高知市, 8 月, **2014**.
2. H. Tooriyama, **E. K. C. Pradeep**, P. Wang, K. Kobiro, Smart decoration of spherical mesoporous TiO_2 nanoparticles with core–shell alloy nanoparticles in supercritical methanol, *4th International Solvothermal and Hydrothermal Association Conference*, Boudreaux, France, October **2014**.
3. **E. K. C. Pradeep**, H. Tooriyama, P. Wang, K. Kobiro, Ultimately simple and smart synthesis of new mesoporous nanoparticles in supercritical methanol, *4th International Solvothermal and Hydrothermal Association Conference*, Boudreaux, France, October **2014**.
4. **E. K. C. Pradeep**, T. Habu, H. Tooriyama, M. Ohtani, K. Kobiro, Fabrication of CeO_2–ZrO_2 mixed spherical mesoporous nanoparticles into homogeneous, domain, and core-shell structures, *4th International Solvothermal and Hydrothermal Association Conference, Boudreaux*, France, October **2014**.
5. **E. K. C. Pradeep**, M. Ohtani, K. Kobiro, One-pot Single-step Synthetic Approach to Morphology Controlled Binary Metal Oxide Nanospheres, *Kochi University-Kochi University of Technology Joint Seminar of Chemistry*, Kochi, Japan, June **2015**.
6. **E. K. C. Pradeep**, M. Ohtani, K. Kobiro, One-pot, single-step, and template free synthesis of mesoporous spherical composite metal oxide nanoparticles in supercritical alcohols, *2nd Annual International Conference on Nanoscience and Nanotechnology–2015*, Colombo, Sri Lanka, September **2015**.
7. M. Ohtani, **E. K. C. Pradeep**, K. Kobiro, Single-step one-pot synthesis of metal oxide composite hollow assemblies, *IUPAC 11th International Conference on Novel Materials and their Synthesis*, Qinhuangdao, China, October 2015.
8. M. Ohtani, **E. K. C. Pradeep**, K. Kobiro, Synthesis of novel spherical porous metal oxide composite nanoassemblies, *IUPAC 11th International Conference on Novel Materials and their Synthesis*, Qinhuangdao, China, October **2015**.
9. **E. K. C. Pradeep**, M. Ohtani, K. Kobiro, One-pot synthesis of hollow porous composite nanoassemblies based on binary metal oxides, *高知工科大学総合研究所 ナノテク研シンポジウム*, 11 月, **2015**.

Patent

1. 特願 2014-214856 号,
   メソポーラスナノ球状粒子製造方法,
   小廣和哉, 大谷政孝, エラワラ・カンカナムゲ・チャンディマ・プラディープ.

Awards

1. *Journal of Supercritical Fluids* "*Editor-in-chief's Featured Article*" award,
   E. K. C. Pradeep, T. Habu, H. Tooriyama, M. Ohtani, K. Kobiro,
   Ultra-simple synthetic approach to the fabrication of CeO_2–ZrO_2 mixed nanoparticles into homogeneous, domain, and core–shell structures in mesoporous spherical morphologies using supercritical alcohols, *J. Supercrit. Fluids* **2015**, *97*, 217–223.
2. ポスター賞,
   E. K. C. Pradeep, M. Ohtani, K. Kobiro,
   One-pot synthesis of hollow porous composite nanoassemblies based on binary metal oxides, *高知工科大学総合研究所 ナノテク研シンポジウム*, 11 月, **2015**.

Miscellaneous

1. **E. K. C. Pradeep**, H. M. P. C. K. Herath, H. R. Perera, C. Li, D. P. Dissanayake, Comparison of polyaniline and polypyrrole based humidity sensors, *The 4th International Symposium on Frontier Technology*, Shenyang, China, August **2013**.
2. X. Li, **E. K. C. Pradeep**, D. Wang, T. Kawaharumura, N. Nitta, H. Furuta, A. Hatta, C. Li, Development of well-aligned ZnO nanorods as photo electrode for dye-sensitized solar cell application, *28th European Photovoltaic Solar Energy Conference and Exhibition*, Frankriech, France, October **2013**.
3. **E. K. C. Pradeep**, X. Li, T. Kawaharamura, D. Wang, A. Hatta, C. Li, Arrayed ZnO Nanorods Fabrication on ZnO Film by Self-catalyst Growth Method in Aqueous Solution, *MRS Online Proc. Libr.* **2014**, *1584*, jsapmrs13-1584-6687.
4. C. Li, X. Li, **E. K. C. Pradeep**, T. Kawaharamura, ZnO thin film phosphor prepared on different substrates by novel multiple reducing annealing, *Dig. Tech. Pap.-Soc. Inf. Disp. Int. Symp.* **2014**, *45*, 1305–1308.